EBioMedicine 000 (2020) 103104

Contents lists available at ScienceDirect

EBioMedicine

journal homepage: www.elsevier.com/locate/ebiom

Persistence of viral RNA, pneumocyte syncytia and thrombosis are hallmarks of advanced COVID-19 pathology

Rossana Bussani[a,1], Edoardo Schneider[b], Lorena Zentilin[b], Chiara Collesi[a,b], Hashim Ali[c], Luca Braga[b,c], Maria Concetta Volpe[b], Andrea Colliva[b], Fabrizio Zanconati[a], Giorgio Berlot[a], Furio Silvestri[a], Serena Zacchigna[a,b,1,*], Mauro Giacca[a,b,c,1,*]

[a] Department of Medical, Surgical and Health Sciences, University of Trieste, 34127 Trieste, Italy
[b] International Centre for Genetic Engineering and Biotechnology (ICGEB), 34149 Trieste, Italy
[c] King's College London, British Heart Foundation Centre of Research Excellence, School of Cardiovascular Medicine & Sciences, SE5 9NU London, United Kingdom

ARTICLE INFO

Article History:
Received 23 September 2020
Revised 8 October 2020
Accepted 15 October 2020
Available online xxx

Keywords:
COVID-19
Post-mortem analysis
SARS-CoV-2
Syncytia
Spike protein
Endothelial dysfunction

ABSTRACT

Background: COVID-19 is a deadly pulmonary disease with peculiar characteristics, which include variable clinical course and thrombophilia. A thorough understanding of the pathological correlates of the disease is still missing.
Methods: Here we report the systematic analysis of 41 consecutive post-mortem samples from individuals who died of COVID-19. Histological analysis is complemented by immunohistochemistry for cellular and viral antigens and the detection of viral genomes by in situ RNA hybridization.
Findings: COVID-19 is characterized by extensive alveolar damage (41/41 of patients) and thrombosis of the lung micro- and macro-vasculature (29/41, 71%). Thrombi were in different stages of organization, consistent with their local origin. Pneumocytes and endothelial cells contained viral RNA even at the later stages of the disease. An additional feature was the common presence of a large number of dysmorphic pneumocytes, often forming syncytial elements (36/41, 87%). Despite occasional detection of virus-positive cells, no overt signs of viral infection were detected in other organs, which showed non-specific alterations.
Interpretation: COVID-19 is a unique disease characterized by extensive lung thrombosis, long-term persistence of viral RNA in pneumocytes and endothelial cells, along with the presence of infected cell syncytia. Several of COVID-19 features might be consequent to the persistence of virus-infected cells for the duration of the disease.
Funding: This work was supported by a King's Together Rapid COVID-19 Call grant from King's College London. MG is supported by the European Research Council (ERC) Advanced Grant 787971 "CuRE" and by Programme Grant RG/19/11/34633 from the British Heart Foundation.

1. Introduction

In December 2019, a novel strain of Coronavirus, named severe acute respiratory syndrome coronavirus-2 (SARS-CoV-2), was isolated from a few patients with COronaVIrus Disease 2019 (COVID-19) by the Chinese Center for Disease Control and Prevention and linked to the cluster of acute respiratory distress syndrome emerging in Wuhan, China [1]. On 30 January 2020, the World Health Organization defined the outbreak of SARS-Cov-2 as an international, public health emergency. Clinical features of patients with COVID-19 indicate that infection with SARS-Cov-2 causes severe, and sometimes fatal, acute lung injury similar to SARS-CoV infection, often requiring intensive care and oxygen therapy [2]. Most patients present with fever, dry cough, dyspnea, and typical bilateral ground-glass opacities on chest CT scans. Over the last couple of months a few studies have explored the lung pathology caused by COVID-19 infection in a small number of patients. The pattern that has emerged is that COVID-19 lung disease causes diffuse alveolar damage (DAD) [3–10], which is also present in other conditions of acute respiratory distress syndrome (ARDS), including SARS.

However, the clinical features of COVID-19 clearly extend beyond those of other causes of ARDS and DAD, in particular to explain the exceptional and persistent severity of the disease in some individuals. Increased levels of proinflammatory cytokines (e.g, IL1B, IL6, IFNγ,

* Corresponding authors at: Department of Medical, Surgical and Health Sciences, University of Trieste, 34127 Trieste, Italy.
E-mail addresses: zacchign@icgeb.org (S. Zacchigna), mauro.giacca@kcl.ac.uk (M. Giacca).
[1] These authors equally contributed as senior authors.

https://doi.org/10.1016/j.ebiom.2020.103104

RESEARCH IN CONTEXT

Evidence before this study

Before undertaking this study, we have considered all work reporting the results of pathological analysis performed on lungs, hearts, kidney, liver and brains from individual infected with SARS-CoV-2, SARS and MERS. We also included publications describing the pathological features of pulmonary damage observed in individuals who died with acute respiratory distress syndrome (ARDS) from causes different from COVID-19 (individuals died before 2019). We have interrogated both Pubmed and Web of Science databases for articles published between January 2003 (year of SARS) and July 2020, searching for the following keywords: SARS, MERS, COVID-19, autopsy, human pathology, DAD, ARDS.

We considered over 150 publications for COVID-19, 56 for SARS and 151 for MERS (also including pathological findings in genetically modified mice expressing the relevant human receptors). The most relevant studies describing the pathological features of SARS, MERS and SARS-CoV-2 infection in comparison to other causes of diffuse alveolar damage are included among the References of our manuscript.

Added value of this study

Our findings add value to the existing evidence as:

i) They derive from the first systematic analysis of multiple organs, considered as potential targets for SARS-CoV-2 infection (lung, heart, brain, kidney and liver), in a large patient cohort (41 individuals). The experience of the pathologist who described these findings (RB), who has performed approximately 600 autopsies/year (at least 100 ARDS/year) over the last 25 years, add further solidity to our findings.
ii) They show persistent presence of the virus in multiple cell types, using both in situ hybridization for viral RNA and immunostaining for the Spike viral protein.
iii) They demonstrate a major involvement of lung endothelial cells, which appear infected and express multiple markers of endothelial dysfunction.
iv) They support the concept that, different from other forms of interstitial pneumonia and ARDS, the clinical features of COVID-19 patients are not attributable to extensive DAD, but rather derive from the persistence of infected and dysfunctional cells in the lung.
v) They demonstrate in a large patient cohort that SARS-CoV-2 infection largely occurs in the lung, with minor involvement of other organs (we did not detect signs compatible with myocarditis, nephritis, hepatitis or encephalitis in any of the analyzed patients).

Implications of all the available evidence

Our study combined with existing evidence indicates that COVID-19 represents a unique pathology, distinct from other causes of ARDS. The long-term persistence of infected cells and the major structural changes detectable in the lungs after several weeks from first diagnosis could represent the anatomical substrate for long-term complications in infected patients who survive the acute phase. Thus, our findings provide a reference for future studies investigating the long-term consequences of SARS-CoV-2 infection.

In addition, the observation of numerous syncytial cells, which likely are the consequence of the fusogenic S-protein of SARS-CoV-2, together with the pathological evidence of endothelial dysfunction, pave the way to future investigations assessing whether the fusogenic SARS-CoV-2-infected cells might be causally linked to the local formation of thrombi.

IP10, and MCP1) have been documented in the blood of patients with extensive lung damage, suggestive of a cytokine storm associated with disease severity [11,12]. After a first phase of viral replication, this inflammatory response was proposed to rapidly amplify even in the absence of significant viral load, resulting in systemic inflammation and eventually leading to multiple organ failure [13]. Diffuse intravascular coagulation and large-vessel thrombosis have been linked to multisystem organ failure, likely associated to hypoxemia in multiple tissues [14]. The lung pathology underlying these severe conditions still remains to be understood. Despite the flurry of anectodical reports on COVID-19 patients' post-mortem analyses over the last couple of months, there is still a paucity of more systematic studies, especially addressing whether a direct connection exists between cell infection by SARS-CoV-2 and the pathology detected.

Several uncertainties still relate to the involvement of other organs in COVID-19. Besides indirect multi-organ injury, a few reports have suggested the possibility of direct injury caused by viral replication in brain, heart and kidney. Mechanistically, SARS-CoV-2 enters the target cells through the interaction of its Spike (S) envelope protein with the angiotensin-converting enzyme-2 (ACE-2) enzyme and upon activation by the TMPRSS2 plasma membrane or by furin proteases [15]. As both ACE2 and TMPRSS2 are broadly expressed in various tissues, including brain, heart and kidney [16] and in light of the similarity with SARS-CoV, which also interacts with ACE2 and had been found in both heart and brain of infected patients [17,18], it was proposed that infection with SARS-CoV-2 could also occur in these organs. A case of encephalitis caused by SARS-CoV-2 was reported in Beijing, with evidence for the presence of viral RNA by genome sequencing in the cerebrospinal fluid [19]. SARS-CoV-2, similar to other SARS coronaviruses, is detectable in the urine via PCR, indicating that kidney tubules are directly exposed to it [20]. Electron microscope particles with SARS-CoV-2 morphology were shown in the kidney epithelium [21]. Despite these anecdotical reports, clear documentation of brain, kidney and heart direct damage caused by the virus is still largely needed.

The systematic analysis of pathology of the lungs and other organs in a large number of COVID-19 patients can provide answers to these outstanding questions. Here were report a large study, performed in 41 consecutive patients who died of COVID-19 at the University Hospital in Trieste, Italy. We provide evidence that COVID-19 causes acute lung injury with distinctive features, including thrombosis of the lung macro- and micro-vasculature, persistence of virus-infected cells the lung pneumocytes and endothelial cells for several weeks from diagnosis and presence of abnormal cell syncytia in the lung in a vast majority of patients. In our patients' cohort, the other organs lacked overt signs of direct viral infection, often in spite of massive alterations in the lungs. We propose that several of the COVID-19 unique features are due to the persistence of abnormal, virus-infected cells in the lungs for prolonged periods of time.

2. Methods

2.1. Case cohort

Histological analysis was performed by expert technicians and pathologists at the Pathology Unit of Trieste University Hospital, which has reached a remarkably high autopsy rate over more than one century (approximately 50% of hospital deaths). In most cases, full body autopsy was performed, which allowed us to analyze lung, brain, heart and kidney tissues. The same pathologists analyzed all samples considered in this study, excluding operator-dependent biases. Clinical data, including age, gender, known co-morbidities and therapies were collected and listed in Table 1 and Supplementary Table 1.

Table 1
Selected clinical and histopathological features.

Case	Gender	Age	Anticoagulant or antiaggregant therapy	Hosp. time (days)	Pneumonia severity	Abnormal pneumocytes	Lung thrombosis	Thrombosis in other organs
Intensive Care								
197.20	M	70	Yes	1	5	+++	Yes	No
207.20	F	76	No	21	4	+++	No	No
210.20	M	73	No	29	5	+++	Yes	No
216.20	M	43	No	21	5*	+++	Yes	No
235.20	M	73	Yes	23	4	+++	Yes	No
262.20	M	82	Yes	18	4	+++	Yes	No
Other hospitalization units								
165.20	M	88	No	14	2#	+	No	No
241.20	F	77	No	3	4	+++	Yes	No
257.20	F	73	No	10	4	+++	Yes	No
272.20	M	80	No	30	5	++	Yes	No
276.20	M	74	Yes	18	5	+++	Yes	Yes§
277.20	M	87	No	8	3	++	Yes	No
285.20	M	73	No	26	3#	++	Yes	No
288.20	F	88	No	28	4#	++	Yes	No
301.20	M	83	No	8	2	+	No	No
302.20	M	71	Yes	60	2	+	No	No
303.20	M	86	No	17	4	++	Yes	No
304.20	M	82	No	9	3	+	No	No
305.20	M	78	No	14	3	+	Yes	No
306.20	M	82	No	24	3	++	Yes	No
307.20	F	86	No	7	4	+++	No	No
308.20	M	85	Yes	6	4	+++	No	No
309.20	F	86	No	5	4	+++	Yes	No
310.20	M	77	No	8	5	+++	Yes	No
311.20	M	85	No	15	4	+	Yes	No
312.20	M	71	No	14	3	++	Yes	No
313.20	M	86	No	17	2	+	No	No
314.20	F	93	No	24	3	+	Yes	No
315.20	F	72	No	28	3	++	Yes	No
316.20	F	88	No	7	2	+	Yes	No
317.20	M	89	No	4	2	+	Yes	No
318.20	M	81	No	2	4#	+	Yes	No
319.20	F	86	No	6	4	+	Yes	No
320.20	M	47	No	13	5	+++	Yes	No
321.20	F	74	No	14	1	-	No	No
322.20	M	72	No	27	5#	+	Yes	No
323.20	F	79	Yes	27	3	+	No	No
324.20	F	97	Yes	14	3#	-	No	No
325.20	F	90	Yes	48	1	-	Yes	No
326.20	F	77	No	3	4#	+	Yes	No
327.20	F	97	Yes	19	2#	+	No	No

Pneumonia severity score:
1, multiple micro-foci of modest inflammation
2, multiple micro-foci of moderate inflammation
3, diffuse moderate inflammation
4, diffuse severe inflammation
5, massive inflammation with loss of lung architecture
* with *ab ingestis* component
# with bacterial component
Abnormal pneumocytes:
+ rare
++ occasional
+++ frequent
§ thromboembolic origin

2.2. Ethics

This study was approved by the Joint Ethical Committee of the Regione Friuli Venezia Giulia, Italy (re. 0019072/P/GEN/ARCS).

2.3. Histology and immunohistochemistry

At least five samples were collected from each organ, selecting representative areas at macroscopic examination. For the lung, three specimens/lobe (two peripheral and one central) were sampled. When evident lesions were present at macroscopic examination, additional sampling was performed, as required. A transversal section of the trachea was also collected.

Samples were fixed in 10% formalin for at least 50 hours and then embedded in paraffin. One-micron sections were processed for the following histological and immunohistochemistry (IHC) staining: hematoxylin-eosin, Azan Mallory, Alcian Blue PAS (ABPAS), colloidal iron, Bluing Reagent (Ventana 760-2037); antibodies against CD4 (790-4423), CD8 (790-4460), CD61 (760-4249), TTF1 (790-4398), CD31 (760-4378), SMA (760-2833) , CD163 (760-4437), Napsin (760-4867) all from Roche; antibodies against Surfactant B (Thermo Fisher Scientific MS-704-P0), HLA-DR (Neomarkers MS-133-P0), SARS-CoV-2 Spike protein (GeneTex GTX632604). Antigen retrieval techniques and antibody pretreatment were performed according to the manufacturer's specifications. Images were acquired using a Leica DM2700 M light microscope.

Please cite this article as: R. Bussani et al., Persistence of viral RNA, pneumocyte syncytia and thrombosis are hallmarks of advanced COVID-19 pathology, EBioMedicine (2020), https://doi.org/10.1016/j.ebiom.2020.103104

2.4. In situ hybridization

In situ hybridization (ISH) was performed in all IC patients (197.20, 207.20, 210.20, 216.20, 235.20 and 262.20) and in five additional patients (241.20, 318.20, 319.20, 323.20 and 325.20), characterized by a short hospitalization time (less than six days), and thus evidence of a positive swab close to their death, and severe lung pathology at histological examination.

ISH was performed using locked nucleic acid (LNA) probes for U6 snRNA (miRCURY LNA Detection probe, Qiagen, cat. no. YD00699002) as previously described [22] and SARS-CoV-2 RNA, designed to target the sense strand of ORF1ab and Spike regions of the viral genome. A scrambled sequence probe (YD00699004) was used as a control. Experiments were performed using a dedicated ISH kit for Formalin-fixed paraffin-embedded (FFPE) tissues (Qiagen) according to the manufacturer's protocol. Briefly, FFPE tissue slides were deparaffinized in xylene, treated with proteinase-K (15 μg/ml) for 5 min at 37 °C and incubated with either SARS-CoV-2 (40 nM) or U6 probes (2 nM) for one hour at 54 °C in a hybridizer. After washing with SSC buffer, the presence of SARS-CoV-2 RNA was detected using an anti-DIG alkaline phosphatase (AP) antibody (1:500) (Roche Diagnostics) supplemented with sheep serum (Jackson Immunoresearch) and bovine serum albumin (BSA). Hybridization was detected by adding NBT-BCIP substrate (Roche Diagnostics). Nuclei were counterstained with nuclear fast red.

We run extensive testing to assess the specificity of our ISH protocol. First, we tested the reactivity of lung samples from different COVID-19-negative individuals to an equimolar mixture of the two COVID-19 probes (representative images for a normal individual and a patient who died of pneumonia due other causes before 2019 are shown in Suppl. Fig. 1 panels a and b). Second, we tested a positive control of hybridisation, consisting of an RNA probe against the ubiquitous U6 small nuclear RNA, which generated positive nuclear signals in all cells (panels c and d). Third, we tested the reactivity of two COVID-19 patients from our cohort to an RNA probe with the same nucleotide content but with a scrambled sequence (panel e); for comparison with a positive SARS-CoV-2 signal, cf. panel f). We have successfully used the same ISH protocol in the past years for experimental purposes in different settings [22].

2.5. Role of funders

Funders were not involved in study design, data collection, data analyses, interpretation or writing the report.

3. Results

3.1. Clinical features

Of the 41 cases considered in our study (25 males and 16 females), 6 required intensive care (IC), while 35 were hospitalized in either other hospital units (Geriatrics n = 12, Infectious Diseases n = 8, Pneumology n = 4, Clinical Medicine n = 2) or local Nurseries (n = 9) until death. The average age of patients was 77 for males and 84 for females. All patients scored positive for SARS-CoV-2 by RT-PCR tests on nasopharyngeal swab and presented symptoms (fever, cough and dyspnea) and imaging data indicative of interstitial pneumonia related to COVID-19 disease. Hypertension (17/41), chronic cardiac disease (13/41), dementia (13/41), diabetes (12/41) and cancer (12/41) were the most common co-morbidities. All patients eventually died of clinical ARDS. Patient data are summarized in Supplementary Table I.

Non-invasive ventilation (NINV) was performed using either helmets or face masks in 20/41 patients. In case of NINV failure, resulting in respiratory acidosis and/or refractory hypoxia despite raising levels of inspired oxygen (FiO_2), fatigue of the respiratory muscles or reduction of the consciousness, patients were admitted to IC for intubation and mechanical ventilation. Patients requiring IC were relatively younger (mean age: 69; age range: 43–82) compared to those hospitalized in other units (mean age: 84; age range: 47–97).

All IC patients received lung-protective respiratory support, consisting in low tidal volume (4–5 ml/kg on ideal body weight), at a lowest FiO_2 able to maintain oxygen saturation (SpO_2) higher than 90%, with positive end-expiratory pressure (PEEP) titrated to keep a driving pressure lower than 14 cm H_20. Respiratory rate was regulated to maintain either carbon dioxide pressure (pCO_2) lower than 55 mmHg or pH higher than 7.2. In patients with a known history of chronic obstructive pulmonary disease (COPD), thresholds were modified to keep pCO_2 as close as possible to patient's usual values. Recruitment manoeuvres were performed at least twice a day both in the prone and in the supine positions. All patients underwent repeated cycles of pronation lasting at least 16 h/day. Two patients received also nitric oxide supplementation.

All IC patients received low molecular weight heparin (LMWH) at therapeutic doses. One patient with suspected pulmonary thromboembolism received both loading and maintenance dose of direct thrombin inhibitors (argatroban, followed by rivaroxaban in combination with LMWH).

3.2. Severe lung damage in COVID-19 patients requiring intensive care

At pathological examination, all cases exhibited lung damage. At macroscopic examination, lungs appeared congested (representative case in Fig. 1A). In 4/41 cases, there was macroscopic appearance of thrombosis of large pulmonary vessels, often with multiple thrombi and in one case determining an extensive infarction in the right lobe (Fig. 1B panels a and b). Histological analysis of all cases revealed gross destruction of the normal lung architecture (shown for representative patients in Fig. 2A panels a–c), consistent with a condition of DAD with edema, intra-alveolar fibrin deposition with hyaline membranes and hemorrhage. This was accompanied by occlusion of alveolar spaces due to cell delamination (panels d–f). Loss of cellular integrity was also confirmed by the presence of nuclear dust, indicative of ongoing cellular death (panel g). Numerous calcified areas were detected throughout the lung parenchyma in 5/41 patients (panel h). The inflammatory infiltrate was relatively modest in most cases (representative picture in Fig. 2B panel a), mainly consisting of clusters of macrophages (panel d), CD8+ lymphocytes (panel b) and less abundant CD4+ cells (panel c).

3.3. SARS-CoV-2 RNA and Spike protein are frequently detected in COVID-19 lungs

We wanted to assess whether the destruction of alveolar tissue and subversion of the lung microarchitecture might be consequent of persisting viral infection, even if several of these patients had died after 30–40 days from diagnosis. We designed two LNA-modified RNA probes for the SARS-CoV-2 genome, hybridizing to the positive strand viral RNA and extensively validated the specificity of our in situ hybridization (ISH) protocol as reported in the Methods section and shown in Supp. Fig. 1. Lung samples from the 6 IC patients and 5 other patients selected for short hospitalization time and severe lung pathology were then analyzed by ISH using the mixture of the two SARS-CoV-2 probes. We detected extensive presence of virus-infected cells in 10/11 of these patients (representative pictures shown in Fig. 2C panels a–d). Hybridisation revealed a significant number of abnormally large and often polynucleated (cf. later) cells showing a large cytoplasm with intense staining for the COVID-19 RNA probe (panels e and f). The detected viral RNA genomes were expressed to form proteins, as concluded from the positivity of several cells to immunohistochemistry using an antibody detecting the viral Spike protein (representative fields in panels g and h). Of note,

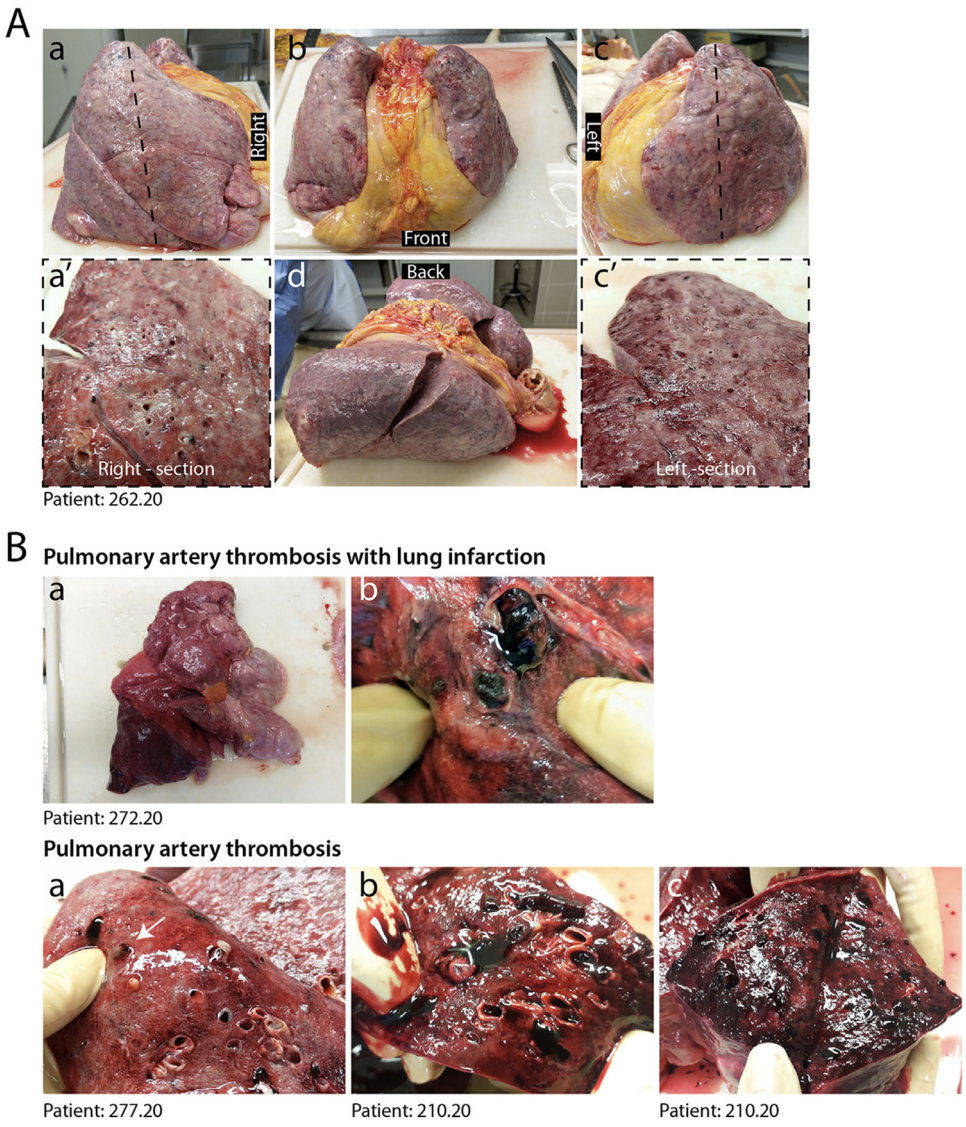

Fig. 1. Macroscopic appearance of COVID lungs. A. Gross appearance of *en bloc* resection of heart and lungs from a severely affected IC patient, shown in its left, anterior, posterior and right views, as indicated (a–d). Lungs appeared congested and firm. Cut sections of both right and left lungs revealed tan-grey solid parenchyma with numerous hemorrhagic areas and loss of air spaces (a', c'). B. A large thrombus in the inferior branch of the right pulmonary artery determined a large infarct in the right lung. Most lungs presented multiple thrombi, with loss of alveolar spaces and extensive hemorrhages (c–e).

several of these dysmorphic, Spike-positive cells showed highly expanded cytoplasms with the presence of large inclusion bodies (panel h).

3.4. Alteration of pulmonary vessels and vascular thrombosis are hallmarks of COVID-19

There were numerous abnormalities in the pulmonary macro- and micro-vasculature in the COVID-19 patients. The presence of perivascular lymphocytic caps, compatible with an ongoing vasculitis, as reported [23,24], was observed in 10/41 patients (24%) and often occurred in thrombotic vessels (Fig. 3A panels a, b and Suppl. Fig. 2A). These inflamed vessels were often characterized by endothelial shedding into the vascular lumen (Fig. 3B). Remarkable vascular defects were observed in one IC individual, in whom numerous vessels of medium and small size were abnormal and stenotic due to massive deformation of their structure (Suppl. Fig. 3). These vessels had an edematous wall, in which smooth muscle cells lost mutual contacts and endothelial cells appeared large, exfoliated and plumped. All three layers were largely inflamed, as revealed by the massive presence of immunoglobulins and HLA-DR-positive leukocytes. In a few cases, the lung parenchyma was infiltrated by numerous megakaryocytes and platelet clusters were present in the thrombi occluding the lung vasculature (cf. later; Suppl. Fig. 2B).

In all the SARS-CoV-2 RNA-positive patients, we found the presence of the viral genome in several of the endothelial cells lining the pulmonary vessels (representative images of ISH from two individuals in Fig. 3C panels a–d). These infected cells were positive for the Spike protein, as shown by immunohistochemistry in Fig. 3D). Infection of endothelial cells by the virus was concomitant with the expression of markers of activation and dysfunction. Several endothelial cells from all the 11 patients tested for the presence of infected cells expressed Tissue Factor (CD142; Fig. 3E and the activation markers E-Selectin (CD62E; Fig. 3F panels a and b) and VCAM-1 (panels c and d).

These alterations of the pulmonary vasculature were concomitant with extensive lung vessel thrombosis, which was detected in 5/6 IC patients (83%) and 16/35 non-IC patients (46%). Thrombi were present in both the micro- and macro-vasculature (Fig. 3G, panels a-h). Thrombi were hetero-synchronous, showed different stages of organization, with some thrombi still infiltrated by inflammatory cells and others in an advanced, fibrotic stage. This is suggestive of

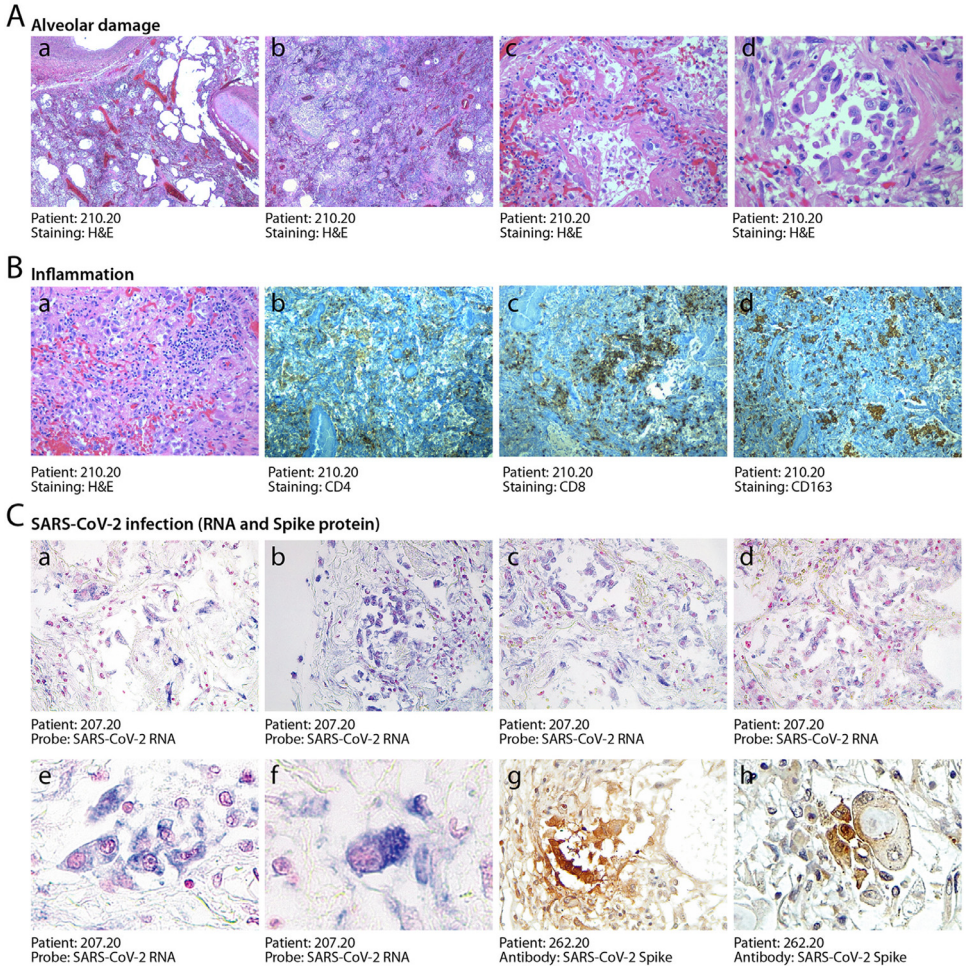

Fig. 2. Histopathological evidence of alveolar damage, inflammation and SARS-CoV-2 infection in COVID-19 lungs. A. Severe and diffuse alveolar damage. Low magnification images (a, b, x2.5) show diffuse end-stage alveolar damage, with patchy inflammatory infiltrates. Higher magnification images better demonstrate massive disruption of alveolar structures and hyaline membranes (c, x20) and detachment of epithelial cells from the alveolar wall (d, x40). B. Moderate inflammatory infiltration. In most patients, lungs were sparsely infiltrated by clusters of inflammatory cells (a, 2.5x), largely composed of $CD4^+$ helper and $CD8^+$ suppressor lymphocytes (b, and c respectively, 2.5x), as well as of $CD163^+$ histiocytes (d, 2.5x). C. Detection of SARS-CoV-2 RNA and Spike protein. In situ hybridization for SARS-CoV-2 RNA revealed extensive positivity in the cytoplasm of several alveolar cells (shown for one representative patient in a-d, x10; e, x20, f, x 40). Cuboidal pneumocytes (g, 20x) and several atypical cells (h, 40x, showing a bi-nucleated cell with a large inclusion body) were also positive for the expression of the Spike protein. Nuclei are stained with nuclear fast red.

endogenous thrombosis in the lung, although we cannot formally exclude repeated embolic episodes. Sporadic lung thrombosis was also present in additional 8/35 of the non-IC patients, for a total of 29/41 (71%) of all the patients that were analyzed.

3.5. *Cytologically abnormal cells are frequent in COVID-19 lung*

An additional pathology characteristic of COVID-19 disease was the presence of anomalous epithelial cells. These were characterized by abnormally large cytoplasm and, very commonly, by the presence of bi- of multi-nucleation (Fig. 4A panels a–f). Presence of these dysmorphic cells was detected in the lungs of 20 patients (50%), including all 6 patients requiring IC, and occasional in additional 16 patients (39%). These cells were present in the alveolar spaces or jutted out into the neighboring, damaged vascular wall. In several instances, these cells clustered to form areas of squamous metaplasia (shown for three patients in Fig. 4B, panels a–c' at two magnifications).

Even more notably, the dysmorphic cells very often showed features of syncytia, characterized by several nuclei with an ample cytoplasm surrounded by a single plasma membrane (Fig. 4C panels a-b' at two magnifications). Most of these syncytia-forming, dysmorphic cells were bona fide pneumocytes, as they resulted positive for surfactant B and napsin, two pneumocyte-specific markers, and expressed the pneumocyte-specific transcription factor TTF1 in their nucleus (Fig. 4D panels a-c respectively). More rarely, these syncytial, giant cells were positive for the CD163 marker, indicating their histiocytic origin (panel d).

Finally, a peculiar and unexpected finding in all the analyzed individuals was the presence of atypical features of bronchial chondrocytes, which were often very large and dysmorphic (Suppl. Fig. 2C panels a/a' and b/b' at two magnifications).

In addition to these COVID-19-specific alterations, the lungs of several patients, especially the elder in the non-IC group, showed signs of pre-existing morbidities, including emphysema and chronic obstructive pulmonary disease. These are reported in Table 1.

3.6. *COVID-19 patients do not show overt signs of viral infection or ongoing inflammation in other organs*

We analyzed the heart, liver and kidney in all IC patients and the brain in three of them. In most cases, these samples presented common features of age-related tissue degeneration, including cardiac fibrosis, liver steatosis, kidney tubular micro-lithiasis, brain gliosis and neuronal loss. However, cellular morphology and tissue integrity were essentially preserved in all the analyzed samples (Suppl. Fig.

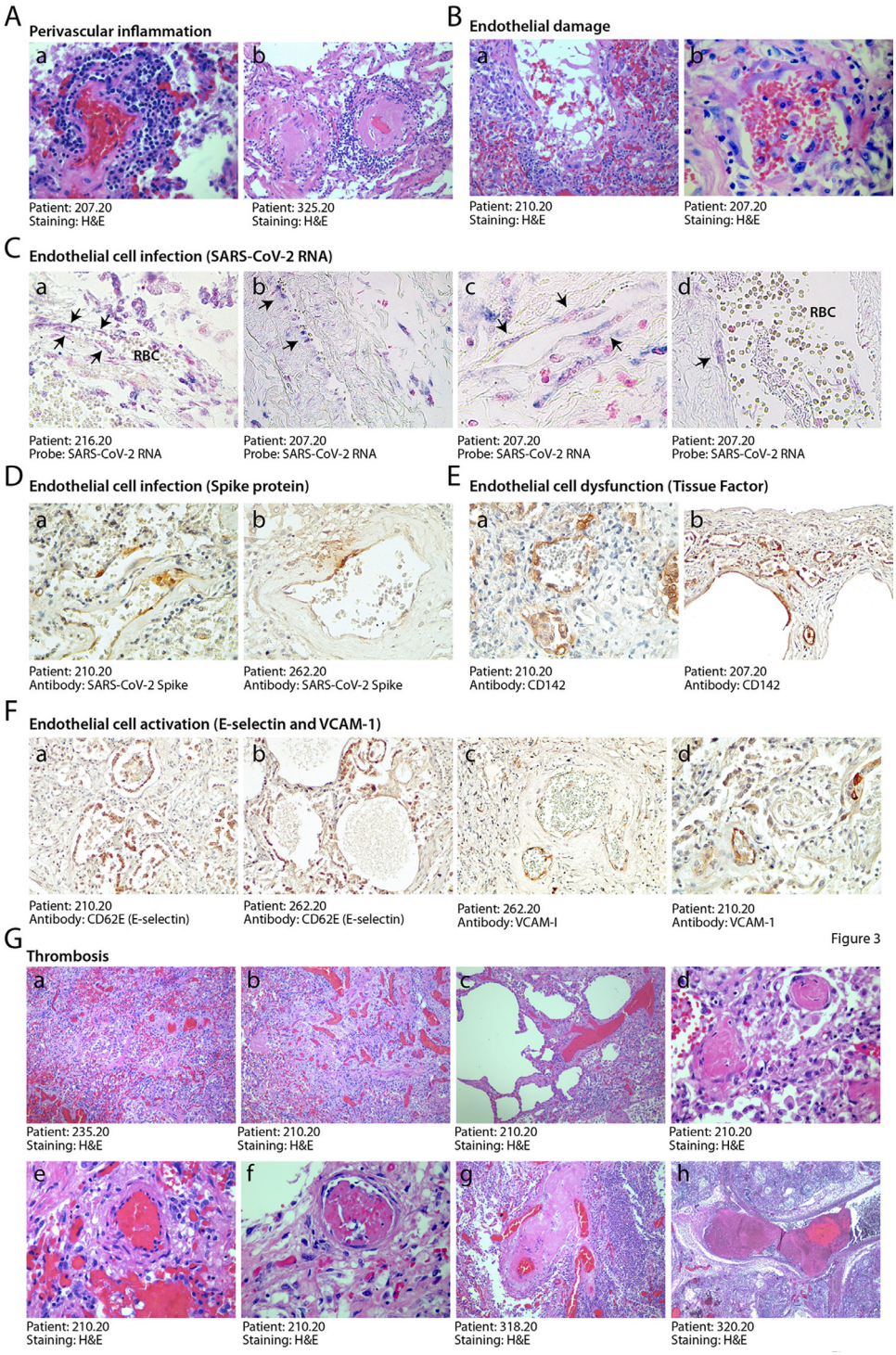

Figure 3

Fig. 3. Endothelial dysfunction and extensive thrombosis in COVID-19 lungs. A. Perivascular inflammation. Numerous patients show clusters of inflammatory cells around small and medium size vessels. In all cases, perivascular lymphocytic cuffs were particularly evident around small arterioles, which had thick walls, often undergoing fibrinoid necrosis (a,b). Other images are in Suppl. Fig. 2A. B. Endothelial damage. Medium and small vessels showed multiple vascular abnormalities, with massive liquefactive degeneration of endothelial cells (a) and their detachment from the vascular wall (b). C. Infection of endothelial cells by SARS-CoV-2. In situ hybridization showing SARS-CoV-2 signal in elongated cells along the luminal side of the vessel wall (arrows), compatible with their endothelial origin (a,b,x10; c, d, x40). RBC: red blood cells. Nuclei are stained with nuclear fast red. D. Expression of the viral Spike protein by endothelial cells. Cells lining blood vessels (shown for a small (a, 10x) and medium (b, 10x) size artery positive for Spike protein. E. Expression of Tissue Factor (CD142). This factor was expressed by the endothelium of several blood vessels of different caliber (a, b, 10x). F. Expression of endothelial cell activation markers. E-selectin (a, b, 10x) and VCAM-1 (c, d, 10x) were expressed in the endothelium of several lung vessels of different caliber. G. Multiple thrombi in different stages of organization. Histological analysis revealed the presence of diffuse micro-thrombi (a, b, x2.5), which sometimes appeared rich in fibrin and poorly organized, consistent with their recent formation (c, x10), but in most instances were largely organized (d, x20). High magnification images confirmed the co-existence of multiple thrombi in different stages of organization in the same lung (a recent thrombus and an organizing thrombus coexist in the lung of the same IC patient, shown in panels e and f, respectively, x20), as well as thrombotic lesions that have likely evolved structurally in multiple times, being composed of an older and a younger component (g, x10; h, x2.5).

Please cite this article as: R. Bussani et al., Persistence of viral RNA, pneumocyte syncytia and thrombosis are hallmarks of advanced COVID-19 pathology, EBioMedicine (2020), https://doi.org/10.1016/j.ebiom.2020.103104

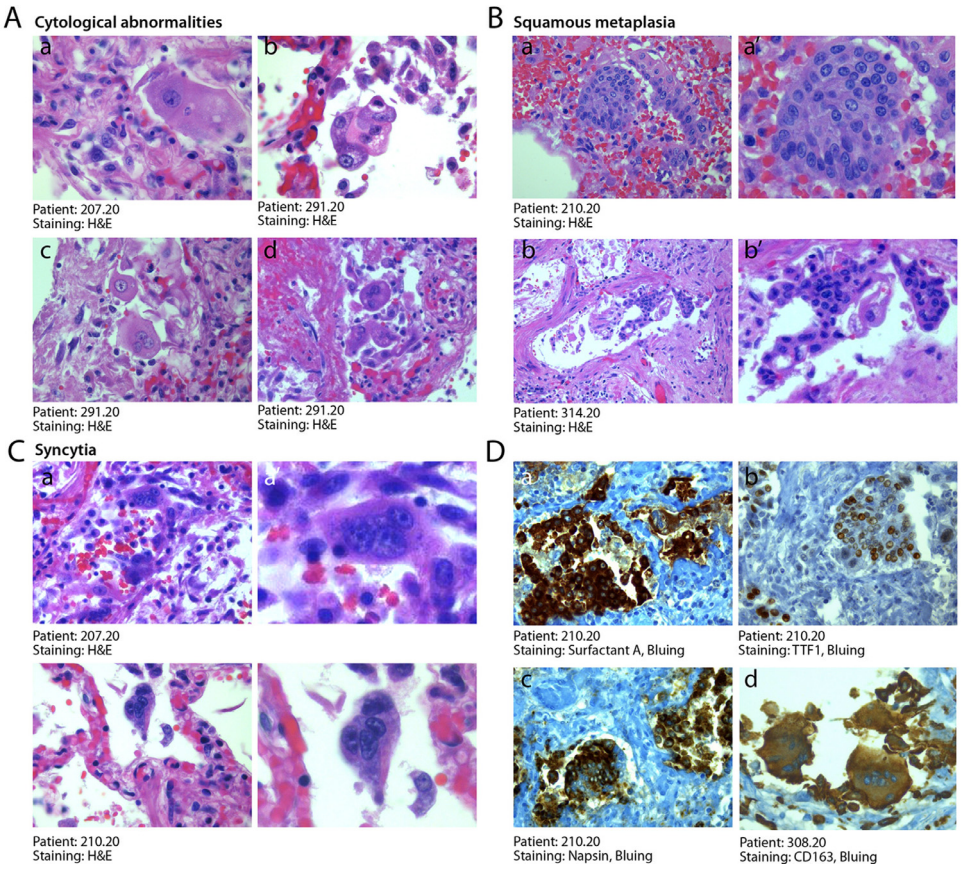

Fig. 4. Abnormal pneumocytes and cellular syncytia in COVID-19 lungs. A. Cytological features of SARS-CoV-2-infected lungs. A consistent and typical feature in COVID-19 lungs was the presence of major cytological abnormalities, including very large cells with dysmorphic phenotypes (a, x63; b, x40) often showing bi-o multinucleation (c,d, x40). B. Squamous metaplasia (pseudosyncytia). A common finding was the metaplasia of the alveolar epithelium, with a marked change in morphology of pneumocytes and their aggregation to form pseudosyncytia (a, b, x20; a', b', x63). C. Syncytia. In addition to squamous metaplasia, true syncytial elements were observed in numerous lungs, showing large cytoplasm and nuclear aggregation (a, b, x20; a', b', x63). D. Origin of syncytial elements. The giant and multinucleated cells forming either pseudo-syncytia or real syncytia scored positive for the pneumocyte markers Surfactant-A (a, x20), TTF1 (b, x20) and Napsin (c, x20), indicative of their epithelial origin. The COVID-19 lungs also showed the more occasional presence of CD163-positive syncytia of histiocytic origin (d, x20). In A-C, H&E: hematoxylin and eosin.

4A–C). We did not detect clear signs of hepatitis, nephritis or encephalitis, such as the presence of massive infiltration of inflammatory cells and/or cytological alterations compatible with direct viral damage. Thrombosis was not detected in any of these organs.

Unspecific signs of age-related pathologies were also common in non-IC individuals. We carefully analyzed the myocardium in additional 19/35 of the non-IC patients. In all the cases, the cardiac tissue showed variable extent of cardiomyocyte damage in both the right and left ventricles, including loss of sarcomeric material and cardiomyocyte anucleation (Suppl. Fig. 4D), often accompanied by fibrosis and amyloid deposition. These pathological features are consistent with the presence of chronic and sustained hypoxia superimposed onto pre-existing damage. No evidence of inflammatory cell infiltration indicative of ongoing myocarditis was evident for any of these patients. However, small vessels positive for the presence of the viral genome were occasionally found in the heart (Suppl. Fig. 4D panel f), along with the sporadic presence of viral RNA also in other cell types (panels g and h). In 12/35 non-IC patients, we also harvested kidney tissue, which often exhibited tubular micro-lithiasis and epithelial necrosis. Also in these cases, no clear signs consistent with viral infection or acute inflammatory disease were observed.

4. Discussion

Here we report the analysis of a series of 41 consecutive patients who died from COVID-19. Our findings add new information on the unique pathology suffered by these individuals and on the extent of viral replication in their lungs.

In the patients who died after prolonged intensive care, alveolar damage was massive, as previous studies have also revealed [3–5,7–10,24–27]. Damage was not dissimilar from that of patients succumbing from ARDS secondary to other conditions, and included detachment of alveolar pneumocytes, deposition of hyaline membranes and marked interstitial edema with advanced fibrotic organization, which are characteristics of advanced DAD from different causes [28,29] including SARS [30]. Besides the lung, we could not detect overt sign of possible viral replication in other organs, including brain, liver, heart and kidney. This is also in agreement with a few very recent studies that investigated kidney [31–33], brain [34,35] and other organ pathology [3,5,36,37] in selected COVID-19 cases. Most of the patients who succumb to COVID-19 have an advanced age and their organs showed variegate signs of age-related comorbidities [38], none of which appears specifically reminiscent of viral infection. This does not exclude, however, that infection of a very few cells in these organs, which have escaped our morphological analysis, would still be a cause for disease. In this respect, it is worth noting that, despite the absence of histological evidence of overt inflammation, we could occasionally detect small vessels and other isolated cells positive for viral RNA in the heart.

Our *in situ* RNA hybridization for the detection of the SARS-CoV-2 genome univocally indicates that the alterations in the lung are concomitant with persistent viral infection of pneumocytes and endothelial cells. RNA-positive pneumocytes were largely present in the

lungs of 10/11 tested individuals. It has been suggested that COVID-19 follows a biphasic course, with an initial phase characterized by viral replication, also detectable by positivity at the RT-PCR-based swab test, followed by second phase in which viral replication might become less relevant, characterized by hyperinflammation. While the clinical manifestations of the disease remain different during disease progression, our data challenge the notion that viral replication has ceased in patients with advanced disease. Expression of the viral nucleocapsid protein was also confirmed in different cell types in the lungs of 7 out 11 examined patients who died of COVID-19 in a recent series [39]. Presence of abundant cytoplasmic RNA signals and expression of the Spike protein in the lungs after 30-40 days from diagnosis in our study suggests ongoing replication and postulates a continuous pathogenetic role of viral infection.

In addition to persistent viral infection, at least two additional hallmarks characterize the COVID-19 pathology. First, the presence of massive lung thrombosis. This was evident at macroscopic examination in 5/6 patients from IC Unit and in 31/41 patients analyzed at the histological level. Fibrin deposition and thrombosis affected both small and large pulmonary vessels and showed clear signs of heterochronicity, with several fresh thrombi neighboring thrombi in advanced stage of organization. This is indicative of a pro-thrombotic process ongoing in the lungs rather than an embolic dissemination event. In terms of defining the underlying cause for thrombosis, we found several endothelial cells lining small and larger vessels infected with the virus. Infection of endothelial cells is rendered possible by the known expression of the ACE2 receptor in these cells [40]. Endothelial cells expression of activation markers, such as VCAM-1 and E-Selectin [41], and of dysfunctional markers such as Tissue Factor (cf. ref. [42] and citations therein) are not specific of COVID-19, as these can be found in other inflammatory and infectious conditions. However, it is tempting to speculate that the extent of these alterations, the concomitant frequent detection of virus-positive endothelial cells and the high rate of thrombosis of COVID-19 patients might be causally related.

The presence of lung thrombosis appears to be a universally recognized feature of COVID-19 disease, as it has been detected by the vast majority of pathology reports over the last couple of months [3,5,9,24,36]. Whether these thrombi can resolve in response to anticoagulant therapy is still matter of debate [43]. In one of our IC patients, who showed transient clinical improvement upon treatment with high dose of anti-coagulants, we could observe an old, organized thrombus detached from the arterial wall, consistent with re-canalization of the vessel (Suppl. Fig. 3D).

Besides persistent viral infection, endothelial dysfunction and lung thrombosis, our study indicates that a third hallmark of COVID-19 disease is the presence of large numbers of dysmorphic cells in the lung. Presence of abnormal pneumocytes [29,44] and syncytial giant cells [45] is also detected in other conditions of DAD, however in a more sporadic and occasional manner. Additionally, most giant cells in other conditions, including SARS, appear to be of histiocytic origin and are not infected by SARS-CoV [46,47], suggesting they derive from the host inflammatory response. While we also sporadically detect such cells in some of our patients (cf., for example, Fig. 4D panel d), most of the atypical cells and syncytia in the COVID-19 patients we analysed instead expressed pneumocyte-specific markers and were positive for SARS-CoV-2 viral RNA. Syncytial elements of pneumocytic origin were also detected in several COVID-19 patients from other very recent studies [7,9,27,48,49]. Thus, the frequent presence of these abnormal cells appears to be characteristic of COVID-19.

We attribute the high prevalence of these syncytial cells to the properties of the SARS-CoV-2 Spike protein. Both SARS-CoV [50] and SARS-CoV-2 [15] bind the ACE2 receptor and can be activated by the TMPRSS2 protease [15,51–53]. However, in the case of SARS-CoV, a main route for Spike activation follows endocytosis of the viral particles and is carried out by endosomal, low pH-activated proteases such as cathepsin B and cathepsin L [54]. In contrast, other proteases, in particular furin, can prime SARS-CoV-2 Spike directly at the plasma membrane level, targeting a sequence at the S1/S2 interface that is not present in SARS-CoV [55,56]. As a consequence, cells expressing SARS-CoV-2 Spike can fuse with other cells expressing the ACE2 receptors and form syncytia, while this property is less pronounced for Spike from SARS-CoV. The possible pathogenetic significance of this difference has remained so far unexplored. Of interest, mice transgenic for the DPP4 MERS-CoV receptor and infected with MERS-CoV develop pulmonary microvascular thrombosis [57]. This observation might hint at the possibility that the fusogenic properties of the MERS-CoV- and SARS-CoV-2-infected cells might be linked to the pathogenesis of thrombosis. Further investigations are needed in this respect.

In light of the persistence of virus-infected cells in the lungs of infected individuals and the peculiar molecular features of the SARS-CoV-2 Spike protein we propose that several of the clinical characteristics that set COVID-19 apart from other interstitial pneumonias are not attributable to pneumocyte death as a consequence viral replication, but to the persistence of virus-infected, Spike-expressing cells in the lungs of the infected individuals.

Contributors

RB: performed post-mortem study and histological analysis, supervised the study
ES: performed in situ hybridisation
LZ: supervised in situ hybridisation
CC: performed immunohistochemistry
HA: designed probes and offered advice on in situ hybridisation
LB: participated in analysis of results
MCV: performed immunohistochemistry
AC: performed immunohistochemistry
FZ: analysed histology
GB: followed patients in ICU
FS: analysed histology
SZ: supervised the study and wrote the manuscript
MG: supervised the study and wrote the manuscript
All authors approved the final version of the manuscript

Data sharing statement

De-identified patient data collected for the study will be rendered available by writing to MG (mauro.giacca@kcl.ac.uk) or SZ (zacchign@icgeb.org).

Declaration of Competing Interest

The authors declare no conflict of interest.

Acknowledgments

This work was supported by a King's Together Rapid COVID-19 Call grant from King's College London. MG is supported by the European Research Council (ERC) Advanced Grant 787971 "CuRE" and by Programme Grant RG/19/11/34633 from the British Heart Foundation.

The authors wish to thank Giacomo Molinari, Katia Di Vito, Sonia De Luca, Marzia Pavlovich, Paola Suligoi, Ida Rosano, Gabriella Slatich and Lorena Ulcigrai for excellent technical support in autopsies, histology and immunohistochemistry. The authors are grateful to Ajay Shah for critical comments and suggestions.

Supplementary materials

Supplementary material associated with this article can be found, in the online version, at doi:10.1016/j.ebiom.2020.103104.

References

[1] Zhu N, Zhang D, Wang W, et al. A Novel Coronavirus from Patients with Pneumonia in China, 2019. N Engl J Med 2020;382(8):727–33.
[2] Tang N, Bai H, Chen X, Gong J, Li D, Sun Z. Anticoagulant treatment is associated with decreased mortality in severe coronavirus disease 2019 patients with coagulopathy. J Thromb Haemost 2020;18(5):1094–9.
[3] Buja LM, Wolf DA, Zhao B, et al. The emerging spectrum of cardiopulmonary pathology of the coronavirus disease 2019 (COVID-19): report of 3 autopsies from Houston, Texas, and review of autopsy findings from other United States cities. Cardiovasc Pathol 2020;48:107233.
[4] Barton LM, Duval EJ, Stroberg E, Ghosh S, Mukhopadhyay S. COVID-19 Autopsies, Oklahoma, USA. Am J Clin Pathol 2020;153(6):725–33.
[5] Fox SE, Akmatbekov A, Harbert JL, Li G, Quincy Brown J, Vander Heide RS. Pulmonary and cardiac pathology in African American patients with COVID-19: an autopsy series from New Orleans. Lancet Respir Med 2020.
[6] Edler C, Schroder AS, Aepfelbacher M, et al. Dying with SARS-CoV-2 infection-an autopsy study of the first consecutive 80 cases in Hamburg, Germany. Int J Legal Med 2020;134(4):1275–84.
[7] Menter T, Haslbauer JD, Nienhold R, et al. Postmortem examination of COVID-19 patients reveals diffuse alveolar damage with severe capillary congestion and variegated findings in lungs and other organs suggesting vascular dysfunction. Histopathology 2020.
[8] Konopka KE, Nguyen T, Jentzen JM, et al. Diffuse Alveolar Damage (DAD) from coronavirus disease 2019 infection is morphologically indistinguishable from other causes of DAD. Histopathology 2020.
[9] Carsana L, Sonzogni A, Nasr A, et al. Pulmonary post-mortem findings in a series of COVID-19 cases from northern Italy: a two-centre descriptive study. Lancet Infect Dis 2020.
[10] Schaller T, Hirschbuhl K, Burkhardt K, et al. Postmortem examination of patients with COVID-19. JAMA 2020.
[11] Mehta P, McAuley DF, Brown M, et al. COVID-19: consider cytokine storm syndromes and immunosuppression. Lancet 2020;395(10229):1033–4.
[12] Zhang X, Tan Y, Ling Y, et al. Viral and host factors related to the clinical outcome of COVID-19. Nature 2020.
[13] Jose RJ, Manuel A. COVID-19 cytokine storm: the interplay between inflammation and coagulation. Lancet Respir Med 2020.
[14] Guzik TJ, Mohiddin SA, Dimarco A, et al. COVID-19 and the cardiovascular system: implications for risk assessment, diagnosis, and treatment options. Cardiovasc Res 2020.
[15] Hoffmann M, Kleine-Weber H, Schroeder S, et al. SARS-CoV-2 cell entry depends on ACE2 and TMPRSS2 and is blocked by a clinically proven protease inhibitor. Cell 2020;181(2) 271-80 e8.
[16] Gheblawi M, Wang K, Viveiros A, et al. Angiotensin-converting enzyme 2: SARS-CoV-2 receptor and regulator of the renin-angiotensin system: celebrating the 20th anniversary of the discovery of ACE2. Circ Res 2020;126(10):1456–74.
[17] Inoue Y, Tanaka N, Tanaka Y, et al. Clathrin-dependent entry of severe acute respiratory syndrome coronavirus into target cells expressing ACE2 with the cytoplasmic tail deleted. J Virol 2007;81(16):8722–9.
[18] Oudit GY, Kassiri Z, Jiang C, et al. SARS-coronavirus modulation of myocardial ACE2 expression and inflammation in patients with SARS. Eur J Clin Investig 2009;39(7):618–25.
[19] Moriguchi T, Harii N, Goto J, et al. A first case of meningitis/encephalitis associated with SARS-Coronavirus-2. Int J Infect Dis 2020;94:55–8.
[20] Soleimani M. Acute kidney injury in SARS-CoV-2 infection: direct effect of virus on kidney proximal tubule cells. Int J Mol Sci 2020;21(9).
[21] Farkash EA, Wilson AM, Jentzen JM. Ultrastructural evidence for direct renal infection with SARS-CoV-2. J Am Soc Nephrol 2020.
[22] Gabisonia K, Prosdocimo G, Aquaro GD, et al. MicroRNA therapy stimulates uncontrolled cardiac repair after myocardial infarction in pigs. Nature 2019;569 (7756):418–22.
[23] Varga Z, Flammer AJ, Steiger P, et al. Endothelial cell infection and endotheliitis in COVID-19. Lancet 2020;395(10234):1417–8.
[24] Ackermann M, Verleden SE, Kuehnel M, et al. Pulmonary vascular endothelialitis, thrombosis, and angiogenesis in Covid-19. N Engl J Med 2020.
[25] Bradley BT, Maioli H, Johnston R, et al. Histopathology and ultrastructural findings of fatal COVID-19 infections in Washington State: a case series. Lancet 2020;396 (10247):320–32.
[26] De Michele S, Sun Y, Yilmaz MM, et al. Forty postmortem examinations in COVID-19 patients. Am J Clin Pathol 2020.
[27] Borczuk AC, Salvatore SP, Seshan SV, et al. COVID-19 pulmonary pathology: a multi-institutional autopsy cohort from Italy and New York City. Mod Pathol 2020.
[28] Kash JC, Taubenberger JK. The role of viral, host, and secondary bacterial factors in influenza pathogenesis. Am J Pathol 2015;185(6):1528–36.
[29] Katzenstein AL, Bloor CM, Leibow AA. Diffuse alveolar damage–the role of oxygen, shock, and related factors. A review. Am J Pathol 1976;85(1):209–28.
[30] Gu J, Korteweg C. Pathology and pathogenesis of severe acute respiratory syndrome. Am J Pathol 2007;170(4):1136–47.
[31] Golmai P, Larsen CP, DeVita MV, et al. Histopathologic and ultrastructural findings in postmortem kidney biopsy material in 12 patients with AKI and COVID-19. J Am Soc Nephrol 2020;31(9):1944–7.
[32] Santoriello D, Khairallah P, Bomback AS, et al. Postmortem kidney pathology findings in patients with COVID-19. J Am Soc Nephrol 2020;31(9):2158–67.
[33] Sharma P, Uppal NN, Wanchoo R, et al. COVID-19-associated kidney injury: a case series of kidney biopsy findings. J Am Soc Nephrol 2020;31(9):1948–58.
[34] Kantonen J, Mahzabin S, Mayranpaa MI, et al. Neuropathologic features of four autopsied COVID-19 patients. Brain Pathol 2020.
[35] Solomon IH, Normandin E, Bhattacharyya S, et al. Neuropathological features of Covid-19. N Engl J Med 2020;383(10):989–92.
[36] Wichmann D, Sperhake JP, Lutgehetmann M, et al. Autopsy findings and venous thromboembolism in patients with COVID-19. Ann Intern Med 2020.
[37] Tian S, Xiong Y, Liu H, et al. Pathological study of the 2019 novel coronavirus disease (COVID-19) through postmortem core biopsies. Mod Pathol 2020;33 (6):1007–14.
[38] Remmelink M, De Mendonca R, D'Haene N, et al. Unspecific post-mortem findings despite multiorgan viral spread in COVID-19 patients. Crit Care 2020;24 (1):495.
[39] Schurink B, Roos E, Radonic T, et al. Viral presence and immunopathology in patients with lethal COVID-19: a prospective autopsy cohort study. Lancet Microbe 2020.
[40] Hamming I, Timens W, Bulthuis ML, Lely AT, Navis G, van Goor H. Tissue distribution of ACE2 protein, the functional receptor for SARS coronavirus. A first step in understanding SARS pathogenesis. J Pathol 2004;203(2):631–7.
[41] Liao JK. Linking endothelial dysfunction with endothelial cell activation. J Clin Invest 2013;123(2):540–1.
[42] Kossmann S, Lagrange J, Jackel S, et al. Platelet-localized FXI promotes a vascular coagulation-inflammatory circuit in arterial hypertension. Sci Transl Med 2017;9 (375).
[43] Bikdeli B, Madhavan MV, Jimenez D, et al. COVID-19 and thrombotic or thromboembolic disease: implications for prevention, antithrombotic therapy, and follow-up. J Am Coll Cardiol 2020.
[44] Beasley MB. The pathologist's approach to acute lung injury. Arch Pathol Lab Med 2010;134(5):719–27.
[45] Rosen DG, Lopez AE, Anzalone ML, et al. Postmortem findings in eight cases of influenza A/H1N1. Mod Pathol 2010;23(11):1449–57.
[46] Nicholls JM, Butany J, Poon LL, et al. Time course and cellular localization of SARS-CoV nucleoprotein and RNA in lungs from fatal cases of SARS. PLoS Med 2006;3 (2):e27.
[47] Gu J, Gong E, Zhang B, et al. Multiple organ infection and the pathogenesis of SARS. J Exp Med 2005;202(3):415–24.
[48] Xu Z, Shi L, Wang Y, et al. Pathological findings of COVID-19 associated with acute respiratory distress syndrome. Lancet Respir Med 2020;8(4):420–2.
[49] Grosse C, Grosse A, Salzer HJF, Dunser MW, Motz R, Langer R. Analysis of cardiopulmonary findings in COVID-19 fatalities: High incidence of pulmonary artery thrombi and acute suppurative bronchopneumonia. Cardiovasc Pathol 2020; 49:107263.
[50] Li W, Moore MJ, Vasilieva N, et al. Angiotensin-converting enzyme 2 is a functional receptor for the SARS coronavirus. Nature 2003;426(6965):450–4.
[51] Glowacka I, Bertram S, Muller MA, et al. Evidence that TMPRSS2 activates the severe acute respiratory syndrome coronavirus spike protein for membrane fusion and reduces viral control by the humoral immune response. J Virol 2011;85(9):4122–34.
[52] Matsuyama S, Nagata N, Shirato K, Kawase M, Takeda M, Taguchi F. Efficient activation of the severe acute respiratory syndrome coronavirus spike protein by the transmembrane protease TMPRSS2. J Virol 2010;84(24):12658–64.
[53] Shulla A, Heald-Sargent T, Subramanya G, Zhao J, Perlman S, Gallagher T. A transmembrane serine protease is linked to the severe acute respiratory syndrome coronavirus receptor and activates virus entry. J Virol 2011;85(2):873–82.
[54] Simmons G, Gosalia DN, Rennekamp AJ, Reeves JD, Diamond SL, Bates P. Inhibitors of cathepsin L prevent severe acute respiratory syndrome coronavirus entry. Proc Natl Acad Sci USA 2005;102(33):11876–81.
[55] Coutard B, Valle C, de Lamballerie X, Canard B, Seidah NG, Decroly E. The spike glycoprotein of the new coronavirus 2019-nCoV contains a furin-like cleavage site absent in CoV of the same clade. Antiviral Res 2020;176:104742.
[56] Hoffmann M, Kleine-Weber H, Pohlmann S. A multibasic cleavage site in the spike protein of SARS-CoV-2 is essential for infection of human lung cells. Mol Cell 2020;78(4) 779-84 e5.
[57] Li K, Wohlford-Lenane C, Perlman S, et al. Middle east respiratory syndrome coronavirus causes multiple organ damage and lethal disease in mice transgenic for human dipeptidyl peptidase 4. J Infect Dis 2016;213(5):712–22.